Uluslararası Mühendislik Araştırma ve Geliştirme Dergisi
International Journal of Engineering Research and Development

UMAGD, (2023) 15(1), 117-124.

10.29137/umagd.1142303

Cilt/Volume:15 Sayı/Issue:1 January/Ocak 2023

Araştırma Makalesi / Research Article

Investigation Of Energy Metabolism In The Different Tissues Of Colon Cancer Xenograft Models Based On The Tca And Cori Cycles And Glycolysis

Hülya Ayar Kayalı[1,2,3*], Esra Bulut Atalay[1,2]

[1] *Izmir International Biomedicine and Genome Institute, Dokuz Eylül University, 35340 Izmir, Turkey*
[2] *Izmir Biomedicine and Genome Center, 35340 Izmir, Turkey*
[3] *Department of Chemistry, Division of Biochemistry, Faculty of Science, Dokuz Eylul University, İzmir 35160, Turkey*

***Başvuru/Received**: 07/07/2022 **Kabul / Accepted**: 28/07/2022 **Çevrimiçi Basım / Published Online:** 31/01/2023*

***Son Versiyon/Final Version**: 31/01/2023*

Abstract

The metabolism is reprogrammed in cancer cells to meet the requirement of their malignant properties. Some specific metabolites can contribute to the malignant transformation in different cancer types. This study aimed to determine the level of glucose, pyruvate, lactate, citrate, alpha-ketoglutarate, D-2-hydroxyglutarate, succinate, fumarate, malate, and oxaloacetate in the different tissues (tumor, colon, brain, and liver) of xenograft models generated by a colon adenocarcinoma cell line (SW480). Glucose and pyruvate levels were determined by the 3,5-dinitrosalicylic acid method and pyruvate assay, respectively. The level of other metabolites was determined by the HPLC analysis. The results show that D-2-HG is highly produced in the tumor tissues (120.2 mg/L), but it could not be detected in liver tissue. In conclusion, TCA and Cori cycles and Glycolysis were investigated in the different tissues of colon cancer xenograft models and found that some metabolites produced tissue-specific.

Key Words

"Colon cancer, xenograft model, targeted metabolomics, metabolite, HPLC"

***Responsible Author: hulya.ayarkayali@gmail.com**

Abbreviations

IDH	*Isocitrate dehydrogenase*
TCA	*tricarboxylic acid cycle*
α-KG	*alpha-ketoglutarate*
D-2-HG	*D-2-hydroxyglutarate*
DNS	*3,5-dinitrosalicylic acid*
DNPH	*2,4-dinitrophenylhydrazine*
MeOH	*methanol*
NaOH	*sodium hydroxide*
H&E	*hemotoxylin and eosin*
HPLC	*high-performance liquid chromatography*
OAA	*oxaloacetate*
AKT	*protein kinase B*
MYC	*Myelocytomatosis*
IBG-AELEC	*Izmir International Biomedicine and Genome Institute Local Ethics Committee for Animal Experiments*

1. Introduction

Colon cancer is the third most frequent malignancy in men and women. According to the new cancer data observed in 2020, colon cancer accounted for 10% of the total cancer incidence and 9.4% of all cancer-related deaths worldwide (Sung et al., 2020). New cases of colon cancer are generally diagnosed in the advanced stages. However, despite technological advancements in the medical field, the 5-year survival rate for late-stage patients has remained unchanged (Siegel et al., 2019). Nowadays, studies about metabolic reprogramming of cancer cells have been increasing to find new therapeutic methods (Neitzel et al., 2020).

Metabolic rearrangement is one of the hallmarks of cancer (Hanahan & Weinberg, 2011). During this process, metabolic pathways are inhibited or activated by mutation, feedback mechanisms, or other factors (DeBerardinis & Chandel, 2016). Significant changes are observed in many pathways, such as Glycolysis and the tricarboxylic acid cycle (TCA) during cancer progression. These pathways can support and/or direct cancer initiation, progression, and treatment response. In addition to energy production, precursors synthesized with TCA intermediates are used for the biosynthesis of amino acids, fatty acids, and nucleic acids, which are the basic building blocks of the cell. Therefore, one of the most critical features of the TCA cycle in dividing cells is its central location for biosynthesis (Martínez-Reyes & Chandel, 2020). In the TCA cycle, the accumulation of some specific metabolites role in the tumorigenesis process. For example, mutant isocitrate dehydrogenase (IDH) enzymes gain neomorphic enzymatic activity and catalyze the conversion from α-KG to 2-Hydroxyglutarate (2-HG). Although the 2-HG level is quite low in normal cells, it accumulates 10-100 times in various cancer types (such as glioma, AML, and colon) and participates in the carcinogenesis process (Du & Hu, 2021).

Metabolism consists of a series of biochemical reactions that provide energy for vital processes to maintain viability and synthesize new biomass. Because they play a role in regulating cellular hemostasis and connecting metabolism to epigenetic alterations, specific metabolites are at the crossroads of metabolism. Therefore, they significantly affect gene expression, cellular differentiation, and tumor microenvironment (Pavlova &Thompson, 2016). Biomarkers are found in cancer and healthy cells and are evaluated as indicators of critical biological and pathological processes. Biomarkers are discovered via metabolomics research, which determines the quantity of metabolites in all metabolic pathways in diverse biological samples. The levels of metabolites produced in only a few metabolic pathways are examined using targeted metabolomics (DeBerardinis & Chandel, 2016). So far, various biomarkers for colon cancer have been discovered in samples such as tissue, serum, and blood, and they have been used in a large variety of applications such as early detection and stage discrimination (Liesenfeld et al., 2015; Qiu, Y., et al., 2014). However, the level of metabolites in the different tissues of a xenograft model has not been investigated until now. This study aimed to determine the concentration of glucose, pyruvate, citrate, α-KG, D-2-hydroxyglutarate, succinate, fumarate, lactate, and malate in the tumor, colon, brain, and liver tissues. Thus, critical biochemical pathways (TCA cycle and Glycolysis) that control mitochondrial energy production were investigated in the different tissues of xenograft models generated by a colon adenocarcinoma cell line (SW480).

2. Material Method

2.1. Cell Line and Animals

A colon adenocarcinoma cell line (SW480) cultured in RPMI-1640 medium was used in this study. The cell culture conditions were applied as described in our previous study (Subasi et al., 2020). The male or female athymic Nude mice ($Foxn1^{nu}$) were used when 6-8 weeks old. The animals were housed in IBG-Vivarium Rodent Facility, and their conditions were 22 ± 2°C, with 12 hours of light/dark periods and access to food and water ad libitum. İzmir International Biomedicine and Genome Institute Local Ethics Committee for Animal Experiments (IBG-AELEC) approved all the conditions, protocol number: 17/2019.

2.2. Xenograft Model Development

Five million SW480 cells were suspended in the growth medium, mixed with matrigel (1:1), and subcutaneously injected into a flank of Nude mice (Chen et al., 2016). The subcutaneous tumor volume was measured with a caliper once a week and calculated with the formula below:

$$\text{Tumor volume} = (\text{length} \times \text{width}^2) \times 0.5 \quad \text{(I)}$$

When the diameter of the tumor reached 1 cm^3, the mice were sacrificed. The tumor, brain, liver, and colon tissues were extracted and stored at -80 °C until metabolite extraction. Some tumor tissue was stored in the 10% formalin to H&E staining.

2.3. Metabolite Extraction from the Xenograft Tissues

The 50-100 mg of liver and brain tissues were grounded in cold %100 methanol (MeOH) (1:5, mg/mL), and colon and tumor tissues were homogenized in chloroform:MeOH: water (2:5:2) in ice for approximately 5 minutes by tissue grinder (NG010). Next, the lysate was incubated in ice for 20 minutes and then centrifuged at 16.000 g for 15 minutes at +4 °C. Next, a vacuum centrifuge was used to remove the supernatant, and the pellet was stored at -80 °C until analysis. Finally, the pellet was resuspended with double distilled water before analysis (Want et al., 2013).

2.4. 3.5-Dinitrosalicylic Acid (DNS) Method

DNS method was used to determine the reduced glucose in the tissues (Miller, 1957). First, the DNS reagent was prepared by dissolving the 1 g of DNS in 20 mL of 2N NaOH and boiled at 95 °C. Next, sodium potassium tartrate (30 g) dissolved in 50 ml of distilled water was slowly added to the DNS reagent, and the final volume was completed to 100 ml with distilled water. Next, the samples and DNS reagent were added 1:1 and mixed at 140 rpm for 10 minutes at 100 °C. Then it was incubated for 1 minute in ice. Finally, the samples and standard glucose solutions (100-4500 mg/L) were measured at 540 nm absorbance.

2.5. Pyruvate Assay

The protocol was adapted to 100 µL (96 well plates) (Yoo et al., 2011). First, the 2,4-dinitrophenylhydrazine (DNPH) solution was prepared by dissolving the 5 mg of DNPH in 5 mL of 2N Hydrochloric Acid (HCl, 37%). Next, to determine pyruvate level, 30 µl of samples and then 10 µl of DNPH solution were added to each well and incubated for 5 minutes at room temperature. Lastly, 60 µl of 2N sodium hydroxide (NaOH) solution was added and incubated again at room temperature for 10 minutes. The samples and standard solutions were measured at 520 nm absorbance.

2.6. Analyzing Metabolites with High-Performance Liquid Chromatography (HPLC) System

The HPLC (Agilent, 1260 Infinity II LC System) system was used for targeted metabolomics analyses. The mobile phase was 9.0 mM H_2SO_4 solution, and the flow rate was 0.4 mL/min. The Alltech OA-1000 column was run at 42 °C. Citrate, α-KG, D-2-hydroxyglutarate, succinate, fumarate, lactate, and malate standards were detected in the UV detector (210 nm). All the HPLC-grade standards were bought from Sigma.

2.7. Hemotoxylin and Eosin (H&E) Staining

Tissue embedding, tissue follow-up, sectioning, and staining protocols were performed as previously described (Fischer et al., 2008). Experiments were carried out by a specialist at Izmir Biomedicine and Genome Center, Histopathology Unit.

2.8. Statistical Analysis

The experiments were carried out three times, and the results are mean ± SD of three independent experiments. The figures were created using GraphPad Prism 8.0 (GraphPad Software, CA, USA).

3. Results

3.1. H&E Staining Results of Tumor Tissues

When the tumor volume reached 1 cm^3 in the xenograft models created from SW480 cells, the mice were sacrificed, and a piece of the tumor tissue was stored in %10 formalin for H&E staining (Figure. 1A). An expert veterinary pathologist evaluated the histopathology results. In the SW480 tumor tissue, tumor parenchyma in the form of islands was observed around the blood vessels (indicated with a yellow arrow). Both anisocytosis and anisonucleosis in tumor cells were moderate. The cell undergoing mitosis was moderately vigorous, and mitotic cells were marked with the red arrow (Figure. 1A).

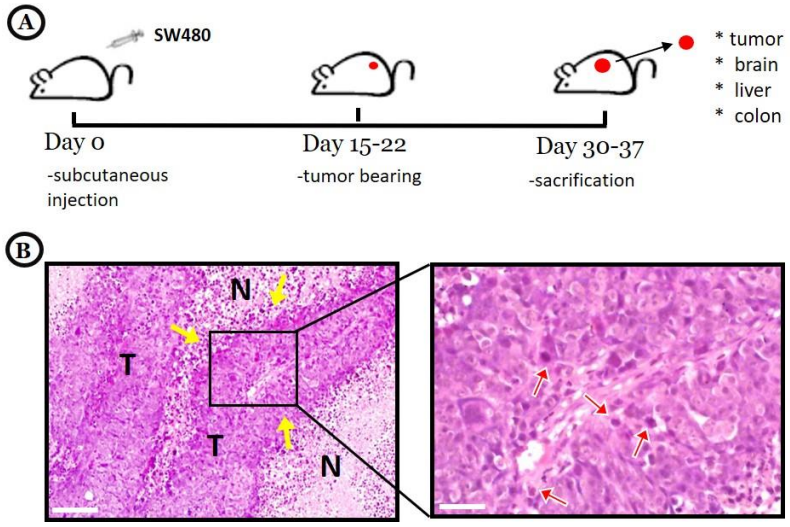

Figure 1. Histopathology Of Xenograft Tumor Tissues. By Subcutaneously İnjecting 5 Million SW480 Cells İnto The Flank Of Male Or Female Nude Mice 6–8 Weeks Old, Xenograft Models Were Generated. **(A)** Representative H&E Staining İmages Of SW480 Tumor Tissue. **(B)** The Right Panel İllustrates Enlargements From The Left Panel (Marked Boxes). The Yellow Arrows İndicate The Borders, And The Red Arrows İndicate The Mitotic Cells. The Scale Bar İs 200 µm.

3.2. Investigating the Metabolite Concentration in the Different Tissues of Xenografts Models

The extracted tumor, brain, liver, and colon tissues from xenografts models were used for metabolite extraction, and the level of glucose, pyruvate, lactate, TCA cycle intermediates, and D-2-HG was estimated.

In the brain tissue, glucose was most metabolized to the TCA cycle than in all other tissues. Related to this, pyruvate level was decreased, and TCA cycle intermediates were more produced. As is seen in Figure 2A, glucose, pyruvate, citrate, α-KG, D-2-HG, succinate, fumarate, malate, and oxaloacetate levels were determined as 112.1, 3.3, 83.3, 78.5, 35.2, 98.9, 40.3, 107.7, 112.3 mg/L in the brain tissues, respectively.

The lowest glucose level was determined in the colon than in all other tissues. (Figure. 2B). The high glucose metabolism led to the increased level of TCA cycle intermediates. The levels of glucose, pyruvate, citrate, α-KG, D-2-HG, succinate, fumarate, malate, and oxaloacetate were determined as 104.1, 3.2, 71.2, 4.6, 11.2, 28, 10, 57.6, 47.4 mg/L in the colon tissues, respectively (Figure. 2B).

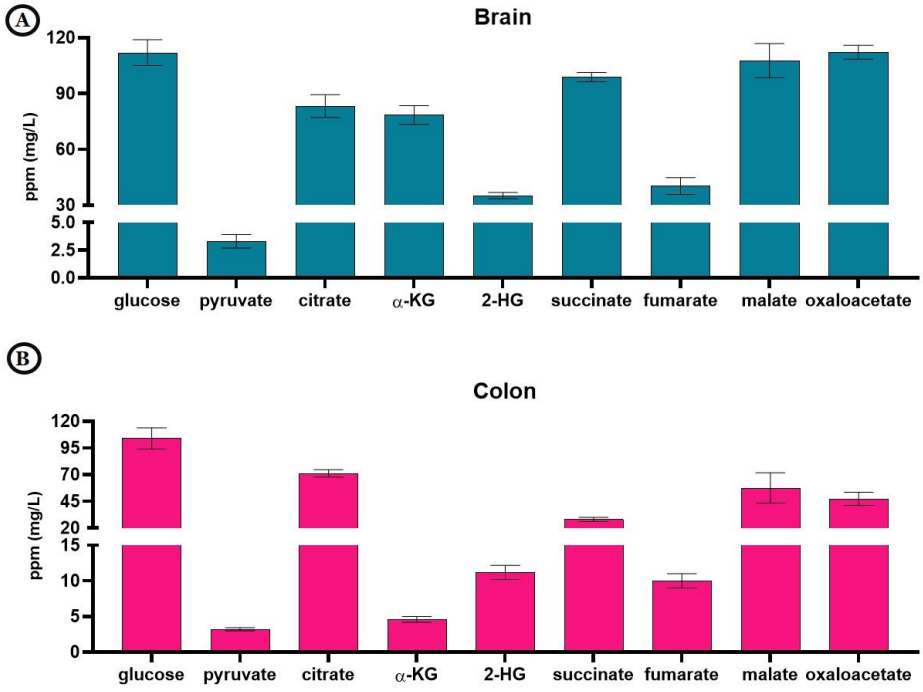

Figure 2. The Metabolites Extracted From The Brain And Colon Tissues Of Xenograft Models Were Generated By A Colon Adenocarcinoma Cell Line. The Level Of Glucose, Pyruvate, Citrate, A-KG, Succinate, Fumarate, Malate, Oxaloacetate, And, D-2-HG Were Determined İn The Brain **(A)** And Colon **(B)** Tissues.

The tumor tissues take more glucose and quickly metabolize it to produce new biomass (Lunt&Vander Heiden, 2011). The results showed that the glucose level was more than the brain and the colon tissues. The levels of glucose, pyruvate, lactate, citrate, α-KG, D-2-HG, succinate, fumarate, malate, and oxaloacetate were determined as 150, 3.8, 70.2, 50.0, 2.4, 120.2, 49.7, 4.1, 22.9, 35.2 mg/L in the tumor tissues, respectively (Figure 3A). Most importantly, the level of D-2-HG was highest in the tumor tissue than in all other tissues.

The glucose and lactate levels were the highest in the liver tissues. The CCD-18Co liver had a very high glucose level (4451,0 g/L). The levels of glucose, pyruvate, lactate, citrate, α-KG, succinate, fumarate, malate, and oxaloacetate were determined as 2173.7, 4.0, 195.7, 43.3, 12.9, 45.7, 2.3, 35.0, 47.3 mg/L in the liver tissue, respectively (Figure 3A). More importantly, D-2-HG was not detected in the liver tissue, revealing that metabolites have produced tissue-specific.

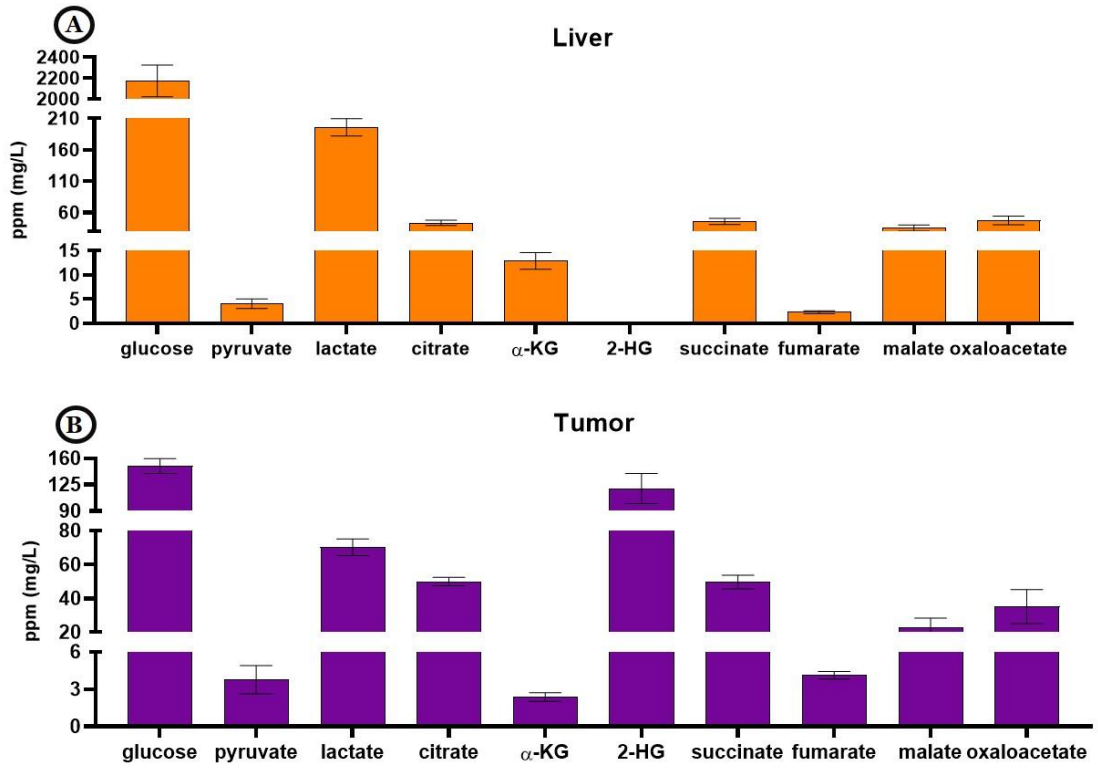

Figure 3. The Metabolites Were Extracted From Liver And Tumor Tissues Of Xenograft Models Generated By A Colon Adenocarcinoma Cell Line. The Level Of Glucose, Pyruvate, Lactate, Citrate, A-KG, Succinate, Fumarate, Malate, Oxaloacetate, And, D-2-HG Were Determined İn The Liver **(A)** And Tumor **(B)** Tissues.

4. Discussion

Cells must adapt to changing metabolic pathways to survive and proliferate in certain conditions (DeBerardinis & Chandel, 2016). Hence, metabolites produced in different forms due to mutations or changing their concentrations are significant therapeutic advantages for scientists. Previous studies showed that the high rate of Glycolysis resulted in a decrease in glucose level and an increase in the level of glycolytic intermediates (Lunt &Vander Heiden, 2011). In our study, the decrease in glucose level in tumor tissues compared to other tissues (Figures 2 and 3) was thought to result from the Warburg effect. On the other hand, glucose level was significantly different in all xenograft tissues. While glucose level in the brain, tumor, and colon tissue decreased, they accumulated in the liver tissues of xenograft models (Figure 4). Genetic analysis shows that the mutations in some glycolytic-enzymes such as the pyruvate kinase, and activation of oncogenes such as protein kinase B (AKT) and Myelocytomatosis (MYC), affect cancer metabolism *in vivo* and lead to dysregulation of glucose metabolism in different tissues (Camarda et al., 2017). We hypothesize that the differences in glucose metabolism in the different tissues can be related to the glycolysis-related enzyme equipment.

In addition to glycolytic intermediates, the synthesis of TCA cycle intermediates is also increased in cancer metabolism. The two different anaplerotic pathways provide an intermediate to the TCA cycle. Glutamine converts to α-KG through the glutaminolysis pathway and participates in the TCA cycle, and pyruvate is converted to oxaloacetate (Dang, 2010; Fan et al., 2009). While the pyruvate level is low in all tissues, the increased oxaloacetate level may be due to the active anaplerotic pathway (Figures 2 and 3). Although the α-KG level is kept in balance with the glutaminolysis pathway, the lowest α-KG level (2.4 mg/L) is determined in tumor tissue. Relatedly, the level of D-2-HG, the reduced form of α-KG, is highest in tumor tissue (Figure 3B; Figure 4).

Lactate, which is highly produced in cancer tissues, can be converted to pyruvate and participate in the TCA cycle, as well as sent to the liver. In this pathway known as the Cori cycle, lactate participates in the gluconeogenesis in the liver tissue, and the glucose produced here is sent back to the cancer tissue (Cori, 1931). In our study, lactate level was lower in tumor tissue compared to liver tissue, and glucose level in liver tissue was found at the highest level compared to other cancer types is consistent with the Cori cycle (Figure 4).

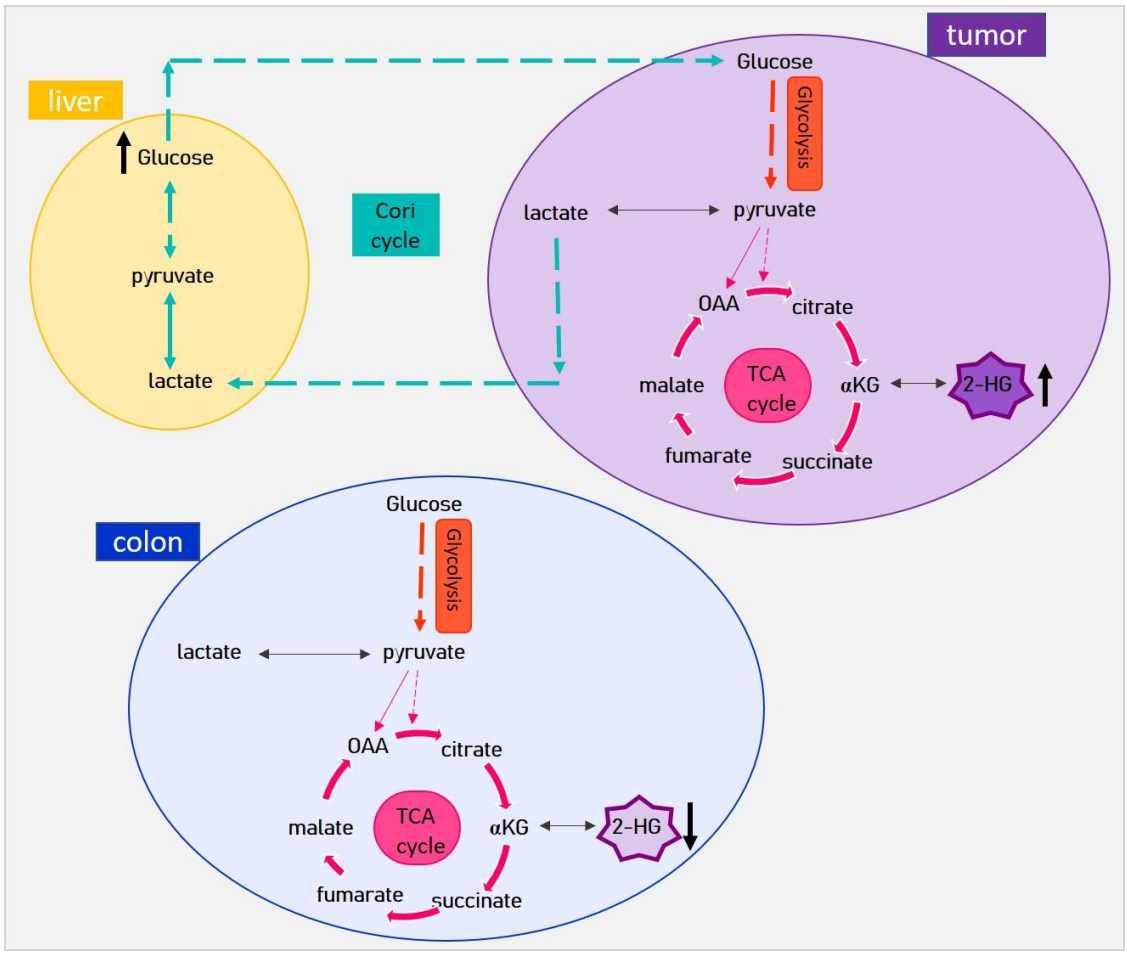

Figure 4. Schematic Presentation Of Metabolic Changes İn The TCA And Cori Cycle And Glycolysis İn The Tumor, Colon, And Liver Tissues Of Xenograft Models. The TCA And Cori Cycles And Glycolysis Are Shown İn Pink, Blue, And Orange, Respectively. A-KG, Alpha-Ketoglutarate; D-2-HG, D-2-Hydroxyglutarate; OAA, Oxaloacetate.

Targeted metabolomics examines the quantities of metabolites produced in specific metabolic pathways (DeBerardinis&Chandel, 2016). In this study, we focus on the metabolite produced in the TCA cycle and Glycolysis. Identifying alterations in metabolite levels is a critical point for the early detection of cancer. Because while some metabolites are produced at a very low level in the healthy cell, they are highly synthesized in the cancer cell and can accumulate to millimolar level. D-2-HG is an example of these oncometabolite. High levels of D-2-HG have been detected in various types of cancer, such as glioma and colon (Du&Hu, 2021). In our study, significant results were obtained for D-2-HG synthesized in all the different tissues. D-2-HG was produced in the brain (35.2 mg/L), colon (11.2 mg/L), and tumor (120.2 mg/L) tissues (Figure 2A-B; figure 3B), whereas it could not be detected in the liver tissue (Figure 3A). The results demonstrated that D-2-HG production is tissue-specific, highlighting the need to use different tissues in metabolomics analyses when analyzing cancer-specific biomarkers. In addition, a 10.7-fold higher D-2-HG level in tumor than in colon tissue (Figures 2 and 3) indicates that this oncometabolite is involved in tumor growth and is consistent with the previous study (Montrose et al., 2012).

5. Conclusion

In this study, how the level of certain intermediates changed in different tissues of xenograft models was investigated. Thus, important pathways that control mitochondrial energy production, such as TCA and Cori cycle, and Glycolysis were investigated besides determining tissue type-specific metabolite levels.

References

Camarda, R., Williams, J., & Goga, A. (2017). In vivo reprogramming of cancer metabolism by MYC. Frontiers in Cell Developmental Biology, 5, 35. doi:10.3389/fcell.2017.00035

Chen, S., Li, X., Chen, R., Yin, M., & Zheng, Q. (2016). Cetuximab intensifies the ADCC activity of adoptive NK cells in a nude mouse colorectal cancer xenograft model. Oncology Letters, 12(3), 1868-76. doi:10.3892/ol.2016.4835
Cori, C.F. (1931). Mammalian carbohydrate metabolism. Physiological Reviews, 11(2),143-275. doi:10.1152/physrev.1931.11.2.143
Dang, C.V. (2010). Glutaminolysis: supplying carbon or nitrogen or both for cancer cells? Cell Cycle, 9(19), 3884-6. doi:10.4161/cc.9.19.13302

DeBerardinis, R. J., & Chandel, N. S. (2016). Fundamentals of cancer metabolism. Science Advances, 2(5), e1600200. doi:10.1126/sciadv.1600200

Du, X., & Hu, H. (2021). The roles of 2-Hydroxyglutarate. Frontiers in Cell and Developmental Biology, 9,486. doi:10.3389/fcell.2021.651317

Fan, T. W. M., Lane, A. N., Higashi, R. M., Farag, M.A., Gao, H., Bousamra, M., & Miller, D. M. (2009). Altered regulation of metabolic pathways in human lung cancer discerned by 13C stable isotope-resolved metabolomics (SIRM). Molecular Cancer, 8(1), 1-19. doi: 10.1186/1476-4598-8-41

Fischer, A. H., Jacobson, K. A., Rose, J., & Zeller, R. (2008). Hematoxylin and eosin staining of tissue and cell sections. Cold Spring Harbor Protocols, 2008(5), 4986. doi:10.1101/pdb.prot073411

Hanahan, D., & Weinberg, R. A. (2011). Hallmarks of cancer: the next generation. Cell, 144(5), 646-674. doi:10.1016/j.cell.2011.02.013

Liesenfeld, D. B., Habermann, N., Toth, R., Owen, R. W., Frei, E., Böhm, J., Schrotz-King, P., Klika Karel, D., & Ulrich Cornelia, M. (2015). Changes in urinary metabolic profiles of colorectal cancer patients enrolled in a prospective cohort study (ColoCare). Metabolomics, 11(4),998-1012. doi:10.1007/s11306-014-0758-3

Lunt, S. Y., & Vander Heiden, M. G. (2011). Aerobic Glycolysis: Meeting the metabolic requirements of cell proliferation. Annual Review of Cell and Developmental Biology, 27(1), 441–464. doi:10.1146/annurev-cellbio-092910-154237

Martínez-Reyes, I., & Chandel, N. S. (2020). Mitochondrial TCA cycle metabolites control physiology and disease. Nature Communications, 11(1),1-11. doi:10.1038/s41467-019-13668-3

Miller, G. L. (1959). Use of dinitrosalicylic acid reagent for determination of reducing sugar. Analytical Chemistry, 31(3), 426-428. doi:10.1021/ac60147a030

Montrose, D.C., Zhou, X.K., Kopelovich, L., Yantiss, R.K., Karoly, E.D., Subbaramaiah, K., & Dannenberg, A. J. (2012). Metabolic profiling, a noninvasive approach for the detection of experimental colorectal neoplasia. Cancer Prevention Research, 5(12), 1358-1367. doi:10.1158/1940-6207.CAPR-12-0160

Neitzel, C., Demuth, P., Wittmann, S., & Fahrer, J. (2020). Targeting altered energy metabolism in colorectal cancer: oncogenic reprogramming, the central role of the TCA cycle and therapeutic opportunities. Cancers, 12(7),1731. doi:10.3390/cancers12071731

Pavlova, N. N., & Thompson, C. B. (2016). The emerging hallmarks of cancer metabolism. Cell Metabolism, 23(1),27-47. doi:10.1016/j.cmet.2015.12.006

Qiu, Y., Cai, G., Zhou, B., Li, D., Zhao, A., Xie, G. Li, H., Cai, S., Xie, D., Huang, C., Ge, W., Zhou, Z., Xu, L. X., Jia, W., Zheng, S.,Yen Y., & Jia W. (2014). A distinct metabolic signature of human colorectal cancer with prognostic potential. Clinical Cancer Research, 20(8), 2136-2146. doi:10.1158/1078-0432.CCR-13-1939

Siegel, R. L., Miller, K. D., & Jemal, A. (2019). Cancer statistics. CA: A Cancer Journal for Clinicians, 69(1), 7-34. doi: 10.3322/caac.21551

Subasi, E., Atalay, E. B., Erdogan, D., Sen, B., AyarKayali, H., & Pakyapan B. (2020). Synthesis and characterization of thiosemicarbazone-functionalized organoruthenium (II)-arene complexes: Investigation of antitumor characteristics in colorectal cancer cell lines. Materials Science and Engineering: C, 106, 110152. doi:10.1016/j.msec.2019.110152

Sung, H., Ferlay, J., Siegel, R. L., Laversanne, M., Soerjomataram, I., Jemal, A., & Bray, F. (2021). Global cancer statistics 2020: GLOBOCAN estimates of incidence and mortality worldwide for 36 cancers in 185 countries. CA: A Cancer Journal for Clinicians, 71(3), 209-249. doi:10.3322/caac.21660

Want, E. J., Masson, P., Michopoulos, F., Wilson, I. D., Theodoridis, G., Plumb, R. S. Shockcor J., Loftus N., Holmes, E., & Nicholson J. K. (2013). Global metabolic profiling of animal and human tissues via UPLC-MS. Nature Protocols, 8(1), 17-32. doi:10.1038/nprot.2012.135

Yoo, K. S., Lee, E. J., & Patil, B. S. (2011). Underestimation of pyruvic acid concentrations by fructose and cysteine in 2, 4-dinitrophenylhydrazine-mediated onion pungency test. Journal of Food Science, 76(8), C1136-42. doi:10.1111/j.1750-3841.2011.02357.x